

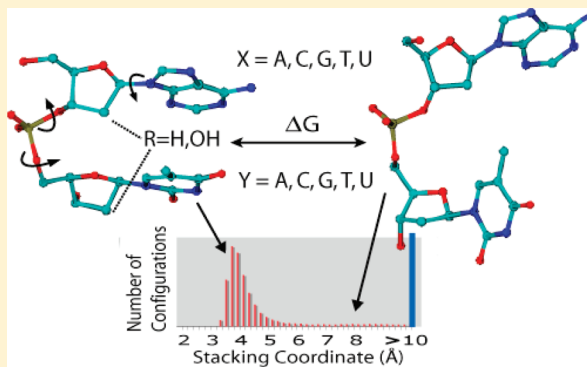
Intramolecular Base Stacking of Dinucleoside Monophosphate Anions in Aqueous Solution

Salem Jafilan, Leah Klein, Christian Hyun, and Jan Florián*

Department of Chemistry, Loyola University Chicago, Chicago, Illinois 60626, United States

Supporting Information

ABSTRACT: Time-dependent motions of 32 deoxyribodinucleoside and ribodinucleoside monophosphate anions in aqueous solution at 310 K were monitored during 40 ns using classical molecular dynamics (MD). In all studied molecules, spontaneous stacking/unstacking transitions occurred on a time-scale of 10 ns. To facilitate the structural analysis of the sampled configurations we defined a reaction coordinate for the nucleobase stacking that considers both the angle between the planes of the two nucleobases and the distance between their mass-centers. Additionally, we proposed a physically meaningful transient point on this coordinate that separates the stacked and unstacked states. We applied this definition to calculate free energies for stacking of all pairwise combinations of adenine, thymine (uracil), cytosine and guanine moieties embedded in studied dinucleosides monophosphate anions. The stacking equilibrium constants decreased in the order 5'-AG-3' > GA ~ GG ~ AA > GT ~ TG ~ AT ~ GC ~ AC > CG ~ TA ~ CA ~ TC ~ TT ~ CT ~ CC. The stacked conformations of AG occurred 10 times more frequently than its unstacked conformations. On the other hand, the last five base combinations showed a greater preference for the unstacked than the stacked state. The presence of an additional 2'-OH group in the RNA-based dinucleoside monophosphates increased the fraction of stacked complexes but decreased the compactness of the stacked state. The calculated MD trajectories were also used to reveal prevailing mutual orientation of the nucleobase dipoles in the stacked state.



INTRODUCTION

Stacking interactions between aromatic bases contribute to stabilization of DNA and RNA secondary structures in aqueous solution¹ and DNA replication fidelity.² The relationships between the chemical properties of nucleobases and their stacking free energies in solution have been thoroughly studied both experimentally^{3–11} and theoretically.^{12–23} In general, base stacking in nucleic acids is a net outcome of a delicate balance of steric, London and electrostatic forces among the bases and the solvent molecules that is subject to conformational constraints imposed by the phosphodiester linkage.^{24–26} Thus, stacking of nucleobases should be studied in the proper biological context, including aqueous solution, counterion, dynamical, and entropic effects.

Previous molecular dynamics (MD) studies of ribo-,^{16,22} and deoxyribodinucleoside monophosphates¹⁷ indicated that their stacking propensity decrease in the order (5'-XpY-3'): purine-purine > purine-pyrimidine > pyrimidine-purine > pyrimidine-pyrimidine^{16,17} and correlated the measured and calculated NMR scalar spin–spin coupling constant to the torsional angles.²² Furthermore, MD and NMR studies of dinucleoside polyphosphates revealed a strong stacking dependence on the length of the backbone.¹¹ Investigation of stacking in the adenosine trimer showed stacking coopera-

tivity,²⁷ but this cooperativity does not seem to involve the electrostatic preorganization.²⁸

In this study, we used classical MD simulations to investigate conformational dynamics of dinucleoside monophosphates (Figure 1) in aqueous solution on a 40 ns time scale. Our examination of the populations of the stacked and unstacked dimer, which is based on a novel definition of the stacking coordinate, yields equilibrium constants for stacking of all 16 deoxyribodinucleoside monophosphates formed by four DNA nucleosides: deoxyadenosine, deoxythymidine, deoxycytidine and deoxyguanosine, and their 16 RNA counterparts from adenosine, cytidine, uridine, and guanosine. Our study provides stacking free energies and activation free energies for unstacking of the dimers and shows that the dipole moments of the bases of d(ApA), d(CpC), d(GpG), and d(TpT) dinucleotides in stacked states self-orient to the twist angle intrinsic to the B-DNA molecule.

METHODS

MD simulations were carried out at a temperature of 310 K in a spherical water droplet of 24 Å radius, which also contained

Received: October 18, 2011

Revised: February 21, 2012

Published: February 27, 2012



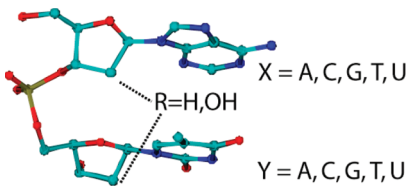


Figure 1. Studied dinucleoside monophosphates; 5'-XY= 5'-d(ApT) is shown as a representative example; hydrogen atoms are not shown.

one Na^+ counterion. Potential energies of solute and solvent molecules were approximated using Amber ff94²⁹ and TIP3P³⁰ molecular mechanical force fields that were implemented in program Q.³¹ Production trajectories of each simulated system were run for 40 ns using 2 fs integration stepsize. The solvent molecules within 3 Å of the edge of the simulation sphere were subjected to spherical boundary conditions^{31,32} designed to mimic bulk solvent.³³ The nonbonding interactions of the atoms of the two stacked nucleobase moieties with the remaining part of the simulated system were explicitly evaluated for all distances. Remaining electrostatic and van der Waals interactions were treated explicitly for distances shorter than 10 Å, whereas for distances longer than 10 Å, a local reaction field (LRF) approximation was used.³⁴ The LRF approximation represents an effective alternative³³ to a more common particle-mesh Ewald method.³⁵

Initial geometries of the stacked ribodinucleoside and deoxyribodinucleoside monophosphate anions were equilibrated for 75 ps with the temperature gradually increasing from 5 to 310 K. Production trajectories of each simulated system were run for 40 ns using 2 fs integration stepsize and SHAKE algorithm. The phosphorus atom was constrained at the center of the simulation sphere using the harmonic potential with a force constant of 50 kcal/mol/Å². One sodium counterion was added to the simulated system to achieve overall zero charge. The distance between the phosphorus and sodium atoms was partly constrained by a flat-bottomed half-harmonic potential to prevent Na^+ ion from entering the area of the sphere subjected to spherical boundary constraints. The flat part of this restraining potential reached from 0 to 20 Å. At these distances the Na^+ ion did not experience any restraining force. Geometries of all atoms and energy data were saved every 400 and 40 fs, respectively.

The issue of overpopulation by the Amber force field of the g^+ t backbone for the α and γ torsional angles in simulations approaching 100 ns³⁶ is known to us. However, our simulation time of 40 ns is much shorter. Although sampling of these torsional angles in the aberrant conformation ($\alpha \approx 100^\circ$ and $\gamma \approx -160^\circ$) did occur during our MD trajectories, these conformations were not sampled exclusively (Figures 1S–4S, Supporting Information).

Stacking free energies were evaluated from the ratio of the number of stacked (N_{stack}) to unstacked (N_{unstack}) configurations as

$$\Delta G = -RT \ln \left(\frac{N_{\text{Stack}}}{N_{\text{Unstack}}} \right) = -RT \ln(K_{\text{Stack}}) \quad (1)$$

where K_{stack} , R , and T are the equilibrium constant for stacking, the universal gas-constant, and thermodynamic temperature. This direct approach of calculating K_{stack} was chosen instead of potential of mean force (PMF) calculations because relatively small activation and “reaction” free energies for the stacking

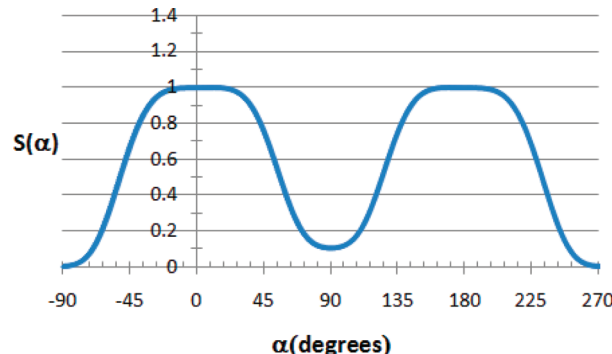


Figure 2. Angular part of the stacking coordinate (eq 3).

process allowed both the stacked and unstacked configurations to be sampled in a single unconstrained MD simulation. The stacking coordinate, ξ , was chosen to be proportional to the vertical distance, R_M , between the centers of mass of the two bases (eq 2).

$$\xi = \frac{R_M}{S(\alpha)} \quad (2)$$

To eliminate T-shaped complexes and to enforce near coplanarity of the stacked bases this distance dependence was modulated by an angular term $S(\alpha)$ (Figure 2).

$$S(\alpha) = e^{-\alpha^4} + e^{-(\alpha-\pi)^4} + 0.1e^{-(\alpha-0.5\pi)^4} \quad (3)$$

where α is an angle (in radians) between the planes of the two bases.

RESULTS AND DISCUSSION

The fraction of stacked nucleobase conformations depends on the definition of the stacked state or, in our case, on the transient value of the reaction coordinate for stacking. A straightforward approach is to define this coordinate as a distance between glycosidic nitrogen atoms of the two neighboring bases (R_{NN}). Norberg and Nilsson, who used this definition in their potential of mean force (PMF) simulations,^{16,17} suggested $R_{NN} = 4.5$ or 5.0 Å to separate the stacked and unstacked states. While the calculated magnitudes of stacking equilibrium constants were affected by this distance, their order for 16 deoxyribonucleotide monophosphates was not.¹⁶

The use of the distance between glycosidic nitrogen atoms as a stacking coordinate oversimplifies stacking behavior of nucleic acids, which exhibit large structural flexibility. Therefore, Sychrovský and co-workers²² included two additional angles in their selection of stacked configurations. In their scheme, only configurations with the angle α between the planes of the two bases of less than 45° were considered as stacked. Additionally, the angle ϕ between the N9-C6 (purine) and N1-C4 (pyrimidine) vectors was required to stay below 60° . The second angular condition eliminated configurations in which one of the bases would flip out of the DNA or RNA strand but remain parallel to the other base. These angular criteria were complemented by a less restrictive distance cutoff of $R_{NN} < 6.4$ Å.

Our design of the stacking reaction coordinate avoids the necessity to limit the angle ϕ by replacing the R_{NN} distance by the distance between the centers of mass of the two bases (R_M). This is because a parallel flipping of a base out of the double-

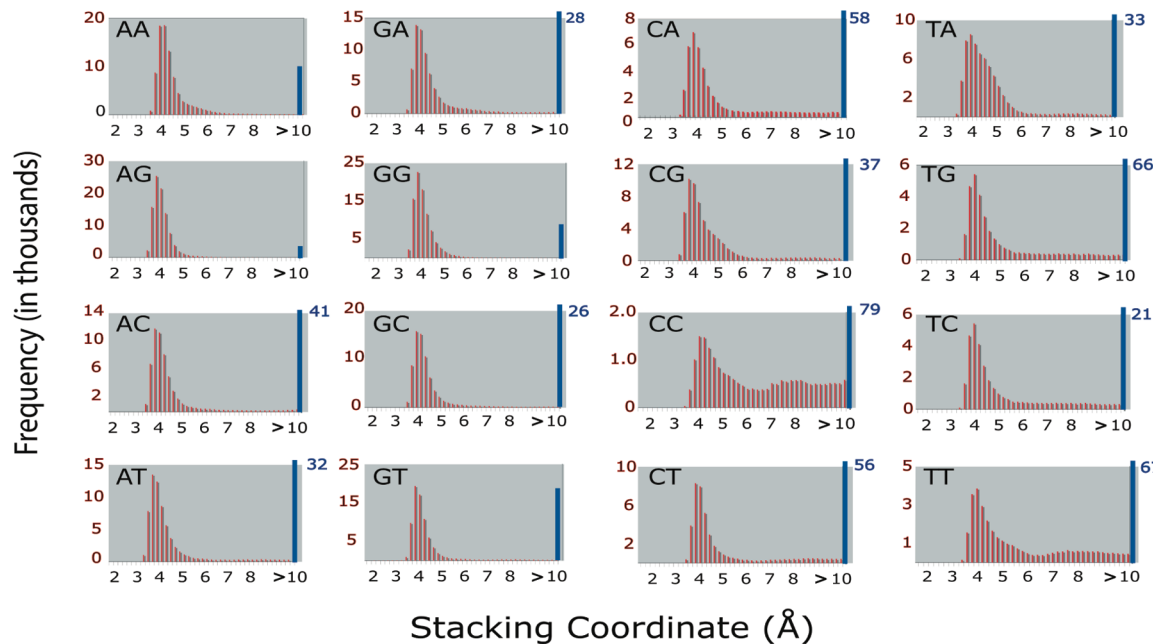


Figure 3. Distribution of the configurations of deoxyribodinucleoside monophosphates in aqueous solution as a function of the stacking coordinate.

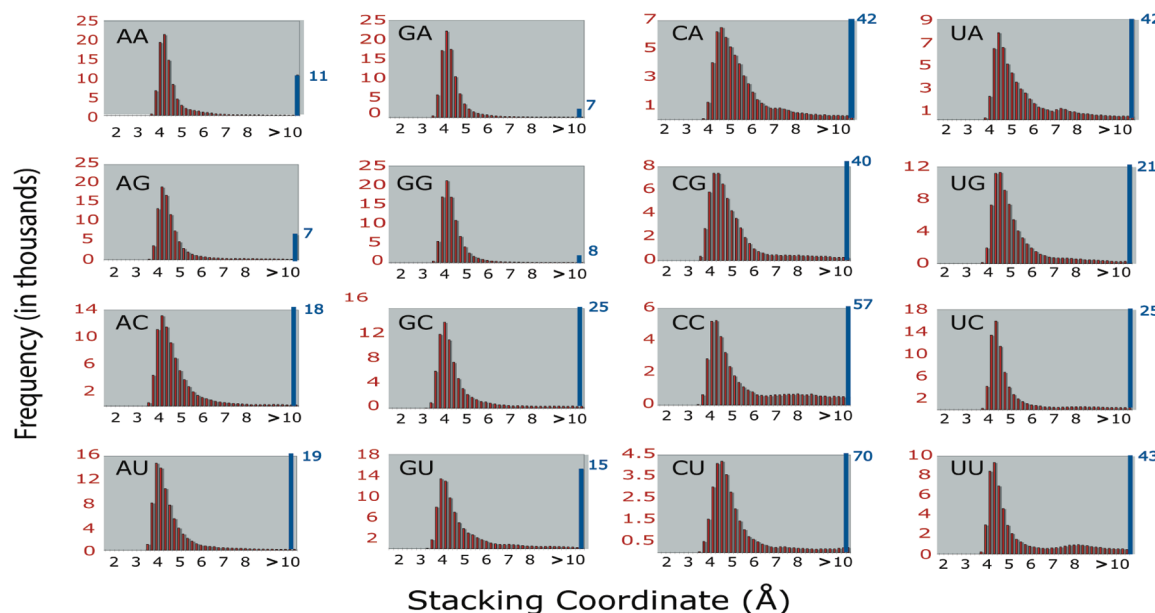


Figure 4. Distribution of the configurations of ribodinucleoside monophosphates in aqueous solution as a function of the stacking coordinate.

helix, which may occur at constant R_{NN} , always increases R_M . In addition, cutoffs in R_{NN} and α were replaced by a function ξ that depends on both R_M and α via eq 2. Because the angular term $S(\alpha)$ (eq 3) has the same broad $S(\alpha) = 1$ plateau near both $\alpha = 0$ and 180° (Figure 2), our stacking function treats equally face-to-face and face-to-back orientations of the two bases. The decrease of $S(\alpha)$ that occurs for nonparallel arrangement of the two bases works alongside the increase in R_M ; both these geometric changes result in larger ξ . Thus, configurations with small and large ξ values correspond to stacked and unstacked conformations, respectively.

The magnitude of ξ fluctuates significantly in the course of simulations as the stacked complexes open and vice versa. We observed at least one opening and closing event for each of the 32 dinucleotides; these time-dependent structural fluctuations

were quantified by counting of each occurrence of a certain ξ value. The resulting histograms of the total number of sampled dinucleotide configurations $N(\xi)$ are presented in Figures 3 and 4. These histograms feature bell-shaped $N(\xi)$ profiles for $3.2 < \xi < 5 \text{ \AA}$, followed by a slower decay in the $5 < \xi < 6 \text{ \AA}$ interval, and a plateau for $\xi > 6 \text{ \AA}$. Since two non-hydrogen atoms that are not covalently bonded are sterically prevented from coming closer than 3.2 \AA , our simulations did not sample any dinucleotide conformation having ξ below this limit. The most tightly stacked conformations are characterized by ξ in the $3.2\text{--}3.4 \text{ \AA}$ range. This ξ range agrees well with the average vertical interbase distance of 3.4 \AA observed in B-DNA crystals.³⁷ However, since a near-perfect vertical alignment of the base mass-centers, yielding $R_M < 3.4 \text{ \AA}$, is a rare event only a small fraction of the calculated configurations have ξ in the

Table 1. Calculated Structural and Thermodynamic Parameters for Base Stacking Interactions in Dinucleoside Monophosphates in Aqueous Solution at 310 K

dinucleotide ^a 5'-XpY-3'	d(NpN) ^b				NpN ^c		
	ξ_{\max}^d	K_{stack}^e	ΔG^f	ΔG_{exp}^g	ξ_{\max}^d	K_{stack}^e	ΔG^f
ApA	3.9–4.1	5.6	-1.1	-1.5 ^h	4.0–4.2	5.8	-1.1
ApC	3.8–4.0	1.1	-0.1	-0.9 ^h	3.8–4.0	3	-0.7
ApG	3.8–4.0	25.2	-2.0	-1.3 ⁱ	4.0–4.2	6.7	-1.2
ApX	3.8–4.0	1.5	-0.3	-0.9 ^h	3.8–4.0	2.9	-0.7
CpA	4.0–4.2	0.5	0.4	j	4.2–4.4	0.9	0.1
CpC	4.1–4.3	0.1	1.3	0.1 ^h	4.1–4.3	0.4	0.6
CpG	3.8–4.0	1.2	-0.1	-0.7 ⁱ	3.9–4.1	1.1	-0.1
CpX	3.8–4.0	0.5	0.4	0.1 ^h	4.2–4.4	0.4	0.6
GpA	3.8–4.0	1.8	-0.4	j	3.8–4.0	9.5	-1.4
GpC	3.8–4.0	2.2	-0.5	j	4.0–4.2	2	-0.4
GpG	3.8–4.0	8.7	-1.3		3.8–4.0	9.1	-1.4
GpX	3.8–4.0	2.9	-0.7		3.8–4.0	2.7	-0.6
XpA	4.0–4.2	1.5	-0.2	j	4.0–4.2	0.9	0.1
XpC	4.0–4.2	0.3	0.6	0.1 ^h	4.0–4.2	1.9	-0.4
XpG	4.0–4.2	2.7	-0.6		4.1–4.3	2.1	-0.5
XpX	4.0–4.2	0.3	0.7	0.1 ^h	4.0–4.2	0.8	0.1

^aX denotes thymine(T) in d(NpN) and uracil(U) in NpN. ^bdeoxyribodinucleoside monophosphates (see also footnote g). ^cribodinucleoside monophosphates. ^dthe range of the stacking reaction coordinate ξ (Å) (eq 2) for which $N(\xi)$ reaches a maximum. ξ_{\max} characterizes the structure of the most stable stacked conformations. ^e $K_{stack} = N(\text{stacked})/N(\text{unstacked}) = N(\xi < 6 \text{ Å})/N(\xi > 6 \text{ Å})$, where $N(\xi)$ is the total number of configurations that have reaction coordinate ξ in the given range. ^fCalculated stacking free energy (kcal/mol) ($T = 298 \text{ K}$, eq 1). By comparing ΔG values obtained from the 20 and 40 ns trajectories (Table 2S, Supporting Information), we estimate that the data presented here are converged to $\pm 0.3 \text{ kcal/mol}$. ^gExperimental free energies at 298 K for the association of 1 M deoxyribonucleosides in aqueous solution.^{7,38} Because monomers were used in these experiments and the measured free energies refer to the formation of various complexes that may have different geometries (stacked or hydrogen-bonded), molecularity, or protonation state, these data provide only qualitative framework for the comparison with the calculated data. ^hThermal osmometry.⁷ ⁱSolubility measurements.³⁸ j $\Delta G_{exp}^g(5'\text{-YpX}) = \Delta G_{exp}^g(5'\text{-XpY})$.

3.2–3.4 Å range. The majority of the stacked conformations occur for ξ in the 3.8–4.4 Å range (Figure 3 and 4), which allows the two bases to slide and tilt with respect to each other. Thus, the conformations in this bin feature average vertical separation between their planes of less than 3.6 Å.

The nucleobase chemical structure alters the stacking histograms to a greater extent than the 2'-substituent (H or OH) on the sugar ring (cf. Figure 3 and 4). On average, the most populated stacked conformations of deoxyribodinucleotides have their ξ values 0.1 Å smaller than the corresponding ribodinucleotides (Table 1). Thus, the 2'-OH group on the sugar seems to be accommodated by a slightly larger slide and tilt of the nucleobases. Judging by the magnitude of N when $N(\xi)$ reaches its maximum (N_{\max}), deoxyribo- and ribodinucleotides have, on average, similar stacking propensity. The T → U substitution has no effect if the other base is adenine (A), it decreases N_{\max} for GT and CT, and increases N_{\max} for TG and TC dinucleotides. In addition, UU stacking was calculated to occur about two-times more frequently than TT stacking. The reduction in the number of stacked TT complexes is probably due to steric repulsion between their 5'-CH₃ groups.

Both TT and UU stacking histograms feature a shallow minimum near $\xi = 6.4 \text{ Å}$. The corresponding activation barrier for unstacking, which can be estimated from the ratio of number of configurations at the $N(\xi)$ maximum and minimum, is about 1.4 kcal/mol at 310 K. Most other dinucleotides do not feature a distinguishable $N(\xi)$ minimum. However, using a value of N at $\xi = 6.4 \text{ Å}$ as a reasonable transition state approximation we can characterize the unstacking of pyrimidine-pyrimidine- and purine-pyrimidine-containing dinucleotides by the activation free energy of 1 to 2 kcal/

mol; a larger activation barrier of about 2 to 3 kcal/mol is characteristic for unstacking of purine-purine dinucleotides.

The presence of the $N(\xi)$ minima or a flat region for $\xi > 6 \text{ Å}$ makes it reasonable to postulate $\xi = 6 \text{ Å}$ as the transient point that separates the pools of the stacked and unstacked configurations. Using this transient point allows us to determine equilibrium constants (K_{stack}) and free energies for stacking (Table 1). The calculated K_{stack} values are only little affected by shifting the transient point on the reaction coordinate from 6 to 7 Å (Table 1S, Supporting Information).

The most stable stacking interaction was calculated for the AG deoxyribodinucleotide (-2 kcal/mol), and GA and GG ribodinucleotides (-1.4 kcal/mol). On the other hand, very weak stacking was obtained for the CC, TC and TT dinucleotides. The large difference between stacking free energies of AG and GA deoxyribonucleotides appears to be structurally related to unfavorable face-to-face geometry (almost no overlap) of nucleobases in GA. In addition, the back-to-face geometries of GA often sample a less advantageous 90° angle between the two nucleobase dipoles (Figure 5).

The purine-purine > purine-pyrimidine > pyrimidine-pyrimidine order of the stacking stability agrees well with the results of ab initio¹⁸ calculations in aqueous solution (Table 2). However, lesser agreement, both in relative and absolute terms, was obtained with the results of PMF calculations of Norberg and Nilsson. Their definition of the transient point ($R_{NN} = 5 \text{ Å}$) yields significantly smaller K_{stack} values because $R_{NN} = 5 \text{ Å}$ corresponds to the position of the maximum of $N(\xi)$.²⁸ However, the smaller K_{stack} calculated for CA ribodinucleotide by us ($K_{stack} = 0.9$) than by Norberg and Nilsson ($K_{stack} = 9.6$) indicates that differences in the MD trajectory lengths employed in these two studies are also significant.

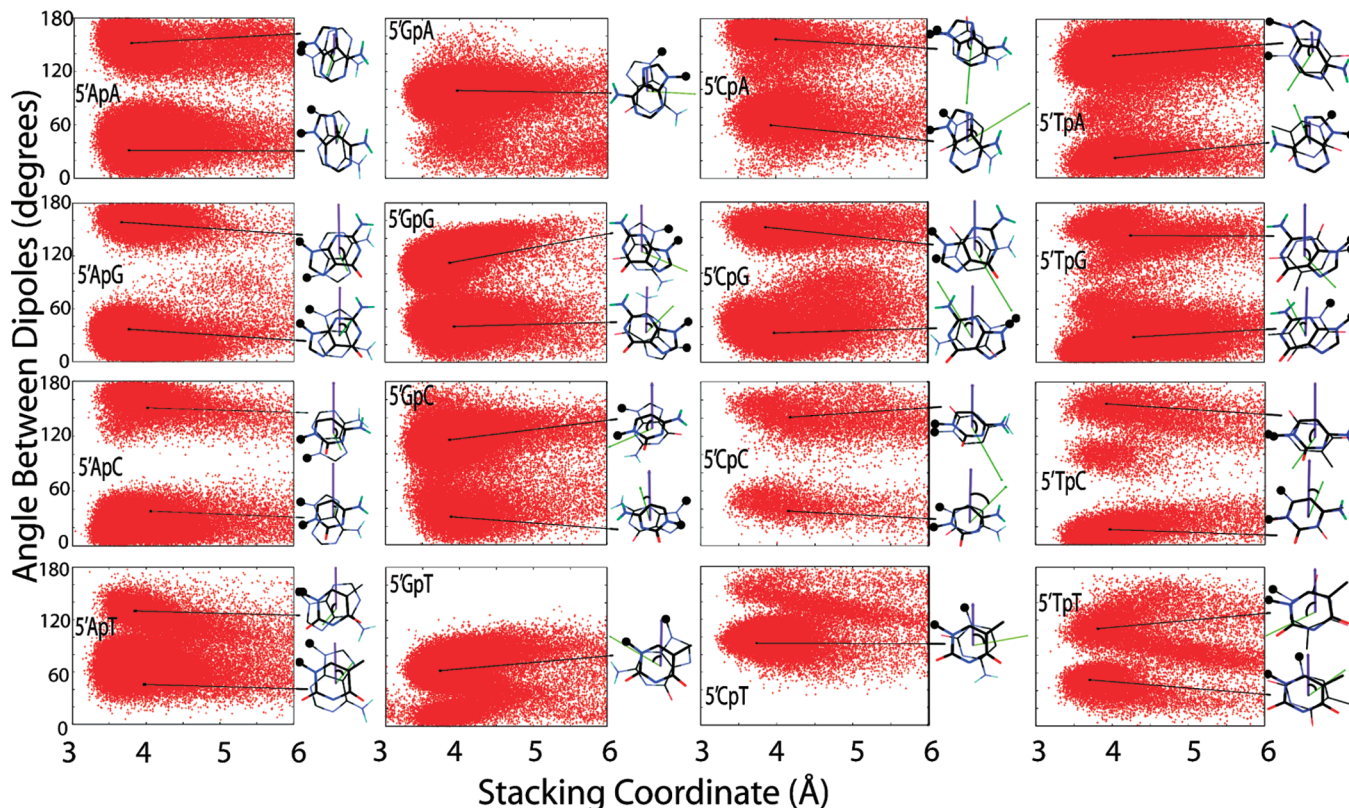


Figure 5. Scatter plots of the angles between dipole moments of nucleobase moieties sampled along a 40 ns MD trajectory. Representative geometries are drawn to the right. The purple and green arrows represent dipole moments of the 3' and 5' base, respectively. The 3'-deoxynucleoside base is outlined more heavily and is placed anterior to the 5' deoxynucleoside base. The sugar-phosphate backbones are symbolized by the solid black circles. Only amino group hydrogens are shown. Dipole vectors, $|\mu(A)| = 0.55 \text{ e}\text{\AA}$, $|\mu(G)| = 1.40 \text{ e}\text{\AA}$, $|\mu(C)| = 1.65 \text{ e}\text{\AA}$, $|\mu(T)| = 1.05 \text{ e}\text{\AA}$, have been scaled by a factor of 3 for illustrative purposes.

Table 2. Comparison of the Calculated Average Free Energies (kcal/mol) for Dinucleoside Monophosphate Stacking in Aqueous Solution

dinucleotide	d(NpN) ^a	NpN ^a	CHARMM ^b	ab initio ^c
5'-purine-purine-3'	-1.2	-1.2	0.2	-0.9
5'-purine-pyrimidine-3'	-0.4	-0.6	-0.1	-0.5 ^d
5'-pyrimidine-purine-3'	-0.1	-0.1	0.0	
5'-pyrimidine-pyrimidine-3'	0.8	0.2	1.4	-0.2

^aPresent simulations, d(NpN) and NpN denote deoxyribo- and ribodinucleoside monophosphates, respectively. ^bPMF calculations of ribodinucleoside phosphates.¹⁶ Equilibrium constants for stacking that were reported by Norberg and Nilsson for $R_{NN} < 5 \text{ \AA}$ stacking condition¹⁶ were converted by us to free energies using eq 1. ^cMP2/6-31+G*/Langevin-dipoles calculations of nucleobase dimers with empirical enthalpy-entropy compensation corrections from DNA melting thermodynamics.¹⁸ ^d5'-3' order of mixed dimers were not distinguished because of the absence of the explicit phosphodiester linkage in the model.

Unfortunately, this theoretical discrepancy cannot be resolved using relevant experiments, because obtaining experimental thermodynamical data for intramolecular stacking of dinucleoside monophosphates has so far presented insurmountable challenge for spectroscopic or calorimetric methods due to low sensitivity of these methods. In fact, it has been easier to determine association thermodynamics for nucleoside monomers (from the observed colligative properties of their aqueous solutions).^{7,38} Interestingly, the calculated free energies are quite close to their experimental counterparts

(Table 1) despite the presence of the phosphodiester linkage, a higher temperature (310 vs 298 K), and a higher effective molarity.

The stacked nucleobases create a net dipole through vector addition of their individual dipoles. According to the Onsager solvation model,³⁹ the solvation free energy of the stacked base-pair is proportional to the square of this net dipole moment. Thus, aqueous solvation tends to stabilize a parallel orientation of the nucleobase dipoles. However, this conformation also results in greater repulsion between the individual dipoles. To minimize this dipole-dipole repulsion, an antiparallel orientation should result. Thus, to lower their total free energy in solution, the dipoles of the nucleobases must orient themselves in order to balance dipole-dipole repulsion of the gas phase and net dipole solvation in water.¹² In balancing these terms, an energetic minimum occurs near a twist angle between the dipoles of the two bases equal to 30° .¹⁸ To include also the effects of the phosphodiester linkages, we examined mutual orientation of dipole moments of the stacked bases (Figure 5). We found that AA, CC, GG, and TT dinucleotides that are stacked in face-to-back orientation favor twist angles between 20° and 60° , the direction that is consistent with the right-handedness of B- and A-DNA. An important role in the preferential stabilizing of these conformations is probably played by both the phosphodiester linkage and electrostatic interactions, whereby contributing to the observed 36° helical rotation per step in B-DNA or 33° rotation in A-DNA. Ab initio investigation of stacking in DNA base-pair steps as a function of angular twist show clear energetic minima around

an average of 34° and 3.5 \AA , in agreement with this study,⁴⁰ although specific sequence can influence the preferred twist angle in the presence of the backbone linker.⁴¹ The observed trend could be further reinforced when polarizable force fields or solutions with higher ionic strengths were considered in explicit simulations.

Base flipping that occurred during the MD simulations of all dinucleotides resulted in two separate populations of twist angles. The face-to-back population features smaller twist angles whereas the larger angles occur for face-to-face or back-to-back stacking arrangement, in which one base is flipped around its glycosidic bond. Two distinct twist-angle populations occur in most dinucleotides with the exception of TA, TG, TC and CA dinucleotides (Figure 5).

In conclusion, past studies have shown that van der Waals or dispersion forces determine the strength of stacking interactions in aqueous solution.^{15,18,42} Our results indicate that electrostatic interactions help to determine the specific twist angle in the stacked complexes. The stacking free energies presented here may serve as benchmarks for calibration of the simplified force fields and solvation models for nucleic acids.

ASSOCIATED CONTENT

Supporting Information

Distribution of α and γ torsional angles of deoxyribodinucleoside and ribodinucleoside monophosphates sampled during a 40 ns simulation trajectory and during the last 500 ps segment of this trajectory and the dependence of the calculated equilibrium constants on the simulation length and the choice of the position of the transition state on the reaction coordinate. This material is available free of charge via the Internet at <http://pubs.acs.org>.

AUTHOR INFORMATION

Corresponding Author

*E-mail: jfloria@luc.edu.

Notes

The authors declare no competing financial interest.

ACKNOWLEDGMENTS

This work was supported by the National Institutes of Health Grant 1U19CA10501 and by the Mulcahy undergraduate research program of Loyola University Chicago.

REFERENCES

- (1) Bloomfield, V. A.; Crothers, D. M.; Tinoco, I., Jr. *Nucleic Acids: Structures, Properties, and Functions*; University Science Books: Sausalito, CA, 2000.
- (2) Kool, E. T. *Annu. Rev. Biophys. Biomol. Struct.* **2001**, *30*, 1.
- (3) Sinanoglu, O.; Abdunur, S. *Photochem. Photobiol.* **1964**, *3*, 333.
- (4) Baker, D.; Marsh, R. E. *Acta Crystallogr.* **1964**, *17*, 1581.
- (5) Chan, S. I.; Schweitzer, M. P.; Ts'o, P. O. P.; Helmkamp, G. K. J. *Am. Chem. Soc.* **1964**, *86*, 4182.
- (6) Broom, A. D.; Schweizer, M. P.; Ts'o, P. O. P. *J. Am. Chem. Soc.* **1967**, *89*, 3612.
- (7) Solie, T. N.; Schellman, J. A. *J. Mol. Biol.* **1968**, *33*, 61.
- (8) Bugg, C. E.; Thomas, J. M.; Sundaralingam, M.; Rao, S. T. *Biopolymers* **1971**, *10*, 175.
- (9) Ts'o, P. O. Bases, nucleosides, and nucleotides. In *Basic principles in nucleic acid chemistry*; Ts'o, P. O., Ed.; Academic Press: New York, 1974; Vol. 1; pp 454.
- (10) Newcomb, L. F.; Gellman, S. H. *J. Am. Chem. Soc.* **1994**, *4993*.
- (11) Stern, N.; Major, D. T.; Gottlieb, H. E.; Weizman, D.; Fischer, B. *Org. Biomol. Chem.* **2010**, *8*, 4637.
- (12) Warshel, A. *J. Phys. Chem.* **1979**, *83*, 1640.
- (13) Danilov, V. I.; Tolokh, I. S. *J. Biomol. Struct. Dyn.* **1984**, *2*, 119.
- (14) Cieplak, P.; Kollman, P. A. *J. Am. Chem. Soc.* **1988**, *110*, 3334.
- (15) Friedman, R. A.; Honig, B. *Biophys. J.* **1995**, *69*, 1528.
- (16) Norberg, J.; Nilsson, L. *J. Am. Chem. Soc.* **1995**, *117*, 10832.
- (17) Norberg, J.; Nilsson, L. *Biophys. J.* **1995**, *69*, 2277.
- (18) Florián, J.; Šponer, J.; Warshel, A. *J. Phys. Chem. B* **1999**, *103*, 884.
- (19) Luo, R.; Gilson, H. S. R.; Potter, M. J.; Gilson, M. K. *Biophys. J.* **2001**, *80*, 140.
- (20) Oostenbrink, C.; van Gunsteren, W. F. *Chem.—Eur. J.* **2005**, *11*, 4340.
- (21) Šponer, J.; Jurečka, P.; Marchan, I.; Luque, F. J.; Orozco, M.; Hobza, P. *Chem.—Eur. J.* **2006**, *12*, 2854.
- (22) Vokáčová, Z.; Buděšínský, M.; Rosenberg, I.; Schneider, B.; Šponer, J.; Sychrovský, V. *J. Phys. Chem. B* **2009**, *113*, 1182.
- (23) Ribeiro, R. F.; Marenich, A. V.; Cramer, C. J.; Truhlar, D. G. *Phys. Chem. Chem. Phys.* **2011**, *13*, 10908.
- (24) Packer, M. J.; Hunter, C. A. *J. Mol. Biol.* **1998**, *280*, 407.
- (25) Šponer, J.; Florián, J.; Ng, H. L.; Šponer, J. E.; Špačková, N. *Nucleic Acids Res.* **2000**, *28*, 4893.
- (26) Norberg, J.; Nilsson, L. *Acc. Chem. Res.* **2002**, *35*, 465.
- (27) Norberg, J.; Nilsson, L. *Biopolymers* **1996**, *39*, 765.
- (28) Bren, U.; Lah, J.; Bren, M.; Martinek, V.; Florián, J. *J. Phys. Chem. B* **2010**, *114*, 2876.
- (29) Cornell, W. D.; Cieplak, P.; Bayly, C. I.; Gould, I. R.; Merz, K. M. Jr.; Ferguson, D. M.; Spellmeyer, D. C.; Fox, T.; Caldwell, J. W.; Kollman, P. A. *J. Am. Chem. Soc.* **1995**, *117*, 5179.
- (30) Jorgensen, W. L.; Chandrasekhar, J.; Madura, J. D.; Impey, R. W.; Klein, M. L. *J. Chem. Phys.* **1983**, *79*, 926.
- (31) Marelius, J.; Kolmodin, K.; Feierberg, I.; Åqvist, J. *J. Mol. Graphics and Modeling* **1999**, *16*, 213.
- (32) King, G.; Warshel, A. *J. Chem. Phys.* **1989**, *91*, 3647.
- (33) Sham, Y. Y.; Warshel, A. *J. Chem. Phys.* **1998**, *109*, 7940.
- (34) Lee, F. S.; Warshel, A. *J. Chem. Phys.* **1992**, *97*, 3100.
- (35) Cheatham, T. E. III; Miller, J. L.; Fox, T.; Darden, T. A.; Kollman, P. A. *J. Am. Chem. Soc.* **1995**, *117*, 4193.
- (36) Pérez, A.; Marchán, I.; Svozil, D.; Šponer, J.; Cheatham, T. E. 3rd; Laughton, C. A.; Orozco, M. *Biophys. J.* **2007**, *92*, 3817.
- (37) Saenger, W. *Principles of Nucleic Acid Structure*; Springer-Verlag: New York, 1984.
- (38) Nakano, N. I.; Igarashi, S. *J. Biochemistry* **1970**, *9*, 577.
- (39) Onsager, L. *J. Am. Chem. Soc.* **1936**, *58*, 1486.
- (40) Cooper, V. R.; Thonhauser, T.; Puzder, A.; Langreth, D. C.; Schroder, E.; Lundqvist, B. I. *J. Am. Chem. Soc.* **2008**, *130*, 1304.
- (41) Samanta, S.; Kabir, M.; Sanyal, B.; Bhattacharyya, D. *Int. J. Quantum Chem.* **2007**, *108*, 1173.
- (42) Packer, M.; Dauncey, M.; Hunter, C. *J. Mol. Biol.* **2000**, *295*.